SAND2017-3608C

ALUMINUM NITRIDE PIEZOELECTRIC MICROPHONES AS ZERO-POWER PASSIVE ACOUSTIC FILTERS

Robert W. Reger[1], Peggy J. Clews[1], Gwendolyn M. Bryan[1,2], Casey A. Keane[1,3], Michael D. Henry[1], and Benjamin A. Griffin[1]
[1]Sandia National Laboratories, Albuquerque, NM, USA
[2]Carnegie Mellon University, Pittsburgh, PA, USA and
[3]University of Florida, Gainesville, FL, USA

ABSTRACT

With the advent of the internet-of-things, sensors that are constantly alert yet consuming near-zero power are desired. Remote sensing applications where sensor replacement is costly or hazardous would also benefit. Piezoelectric micro-electro-mechanical systems (MEMS) convert mechanical or acoustic energy into electrical signals while consuming zero power. When coupled with low-power complementary metal-oxide-semiconductor (CMOS) circuits, a near-zero power sensing system is formed. This work describes piezoelectric MEMS microphones based on aluminum nitride (AlN). The microphones operate as passive acoustic filters by placing their resonant response within bandwidths of interest. Devices are demonstrated with operational frequencies from 430 Hz to greater than 10 kHz with quality factors as large as 3,000 and open-circuit voltages exceeding 600 mV/Pa.

KEYWORDS

Low-power sensors; microphone; piezoelectric; aluminum nitride

INTRODUCTION

The internet-of-things has unplugged our world. The desire to acquire and send information about everything from our heartrates to sensing in remote locations has generated a need for sensors which are both continuously aware and consume near-zero power. Unfortunately, employing current commercial-off-the-shelf (COTS) solutions for these purposes is sub-optimal due to relatively large power requirements.

The typical COTS solution to this problem would require continuous power consumption to be constantly aware, therefore requiring battery replacement or charging with timelines on the order of days (cellphones, heart rate monitors, etc.) to months (remote sensing applications). There exists, therefore, a requirement for near-zero power yet constantly-alert sensors to significantly increase deployment lifetimes. Piezoelectric MEMS offer a solution whose physical transduction mechanism requires zero power and which can be coupled with low-power complementary metal-oxide-semiconductors (CMOS) to form sensing systems.

In this work, we present a piezoelectric MEMS microphone incorporating aluminum nitride (AlN). While AlN's parallel (d_{33}) and transverse (d_{31}) piezoelectric coefficients are 50-100 times lower than lead zirconate titanate (PZT), its low permittivity allows for a higher sensitivity coefficient (g_{31} = 0.027 versus 0.018 V/m/Pa) [1]. This allows for larger open circuit voltages at the same input pressure. AlN also maintains a larger signal to noise ratio than PZT ($21.4\text{x}10^5$ versus $11.7\text{-}20.3\text{x}10^5$ $\text{Pa}^{1/2}$). In addition, AlN is fully CMOS compatible enabling potential on-chip integration with electronics.

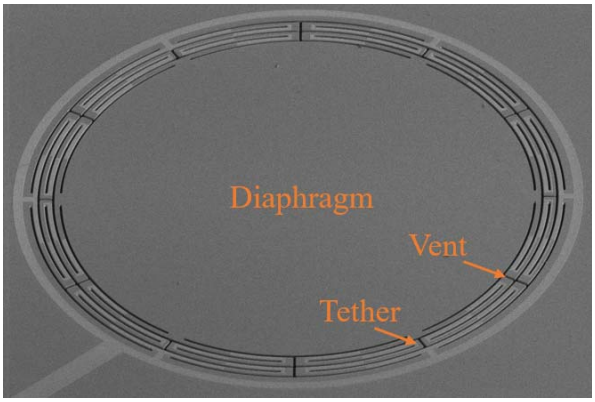

***Figure 1**: Scanning electron microscope image of the resonant microphone. Black areas comprise the vent.*

The MEMS microphone relies on passive piezoelectric transduction of mechanical strain into an electric field. The electric field generates a charge difference between the upper and lower electrodes which is measured as an open circuit voltage across the capacitance. The device designs are resonant about a frequency of interest to improve discrimination to the desired signal. They rely on the piezoelectric effect to convert the mechanical inputs to electrical outputs to obtain near zero power operation.

In the following, we present the device design and discuss the fabrication process used for form the microphone. Then a lumped element model that represents device performance is given. Finally, the device characterization is shown including experiments on a laser vibrometer system and in a plane wave tube.

DESIGN

The microphone consists of a diaphragm suspended from the die by tethers formed from a composite of single crystal silicon (Si), AlN, and an aluminum top electrode as show in Figure 1. The trench etch that forms the tethers creates a vent that equilibrates static pressure between the front and backsides of the diaphragm.

In general, a desirable microphone would maintain a large flat-band response over a broad frequency range of interest as shown in Figure 2. Resonant microphones are designed such that their resonance peak occurs within normal microphone bandwidths at a selected frequency of

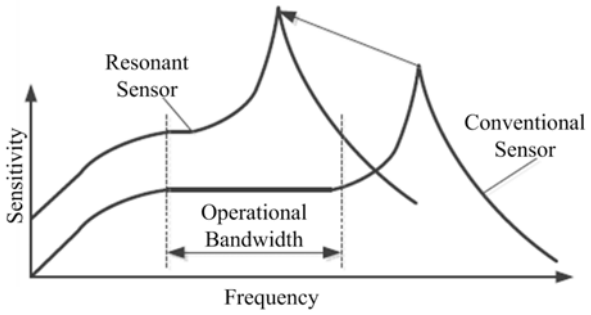

***Figure 2**: Traditional microphone response compared to a resonant microphone response.*

interest. This allows passive filtering of noise and amplification of the desired signal.

FABRICATION

The device fabrication was performed at Sandia National Laboratories in the Microsystems and Engineering Sciences Applications (MESA) complex. The front-end process is shown in Figure 3 and the back-end process is illustrated in Figure 4.

Front End Fabrication Process

(a) Begin with a silicon on insulator (SOI) wafer with a highly doped (1 mΩ-cm resistivity) silicon device layer which will serve as the bottom electrode in the piezoelectric film stack. (b) Deposit a thin 50 nm oxide to serve as an AlN via etch stop and pattern into mesas at the via locations. (c) Reactively sputter deposit a 750 nm AlN film. (d) Etch AlN to form a via stopping on the oxide mesas. (e) Etch oxide via stops using a buffed oxide etch. (f) Deposit and pattern top metal electrode (700 nm aluminum (0.5% copper) and 50 nm titanium nitride). (h) Pattern oxide-hard mask and etch AlN and silicon device layer landing in the buried oxide (BOX). (i) Deposit oxide-hard mask on the wafer backside for back-end of line processing.

Back End Fabrication Process

(j) Pattern the oxide-hard mask on the back of the wafer. (k) Re-pattern the backside of the wafer with photoresist to form a nested mask used to create a thick diaphragm for structural stiffness and mass. (l) Deep reactive ion etch (DRIE) the backside to form the silicon

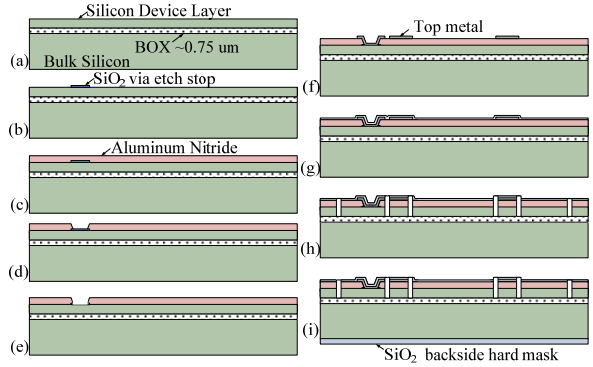

***Figure 3:** Front end of the line fabrication steps as described above.*

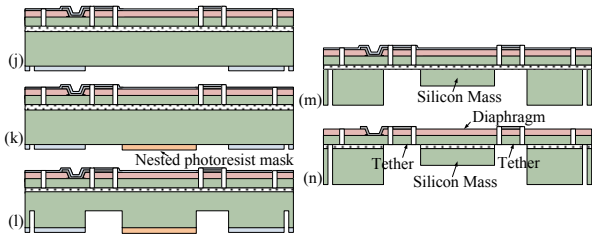

***Figure 4**: Back end of the line fabrication steps as described above.*

diaphragm depth. (m) Remove the nested photoresist mask and continue the DRIE until landing on the BOX. (n) Hydrofluoric acid etch to release the diaphragm.

MODELLING

The device can be described by lumped elements in the acoustic and electrical domains as shown in Figure 5. In the acoustic domain, the tethers are represented by a spring with compliance C_{AD}. The compliance can be derived from composite beam mechanics and is beyond the scope of this document. The tethers are connected to the diaphragm which is represented by mass M_{AD} (determined by the volume and density of materials that compose the diaphragm). In addition, there is mechanical loss, R_{AD}, due to anchor losses, thermoelastic effects, etc., which is most readily extracted from measurements. In addition, there is an impedance due to loading of the fluid surrounding the diaphragm. The fluid that moves in contact with diaphragm is represented by a mass, M_{rad}. The re-radiation of acoustic waves into the fluid is a loss mechanism represented by R_{rad} [2]. The gaps around the tethers create a vent with acoustic resistance, R_{AV}. The back cavity is represented by a spring with compliance C_{AC} estimated by [2],

$$C_{AC} = \frac{V}{\rho_0 c_0^2} \tag{1}$$

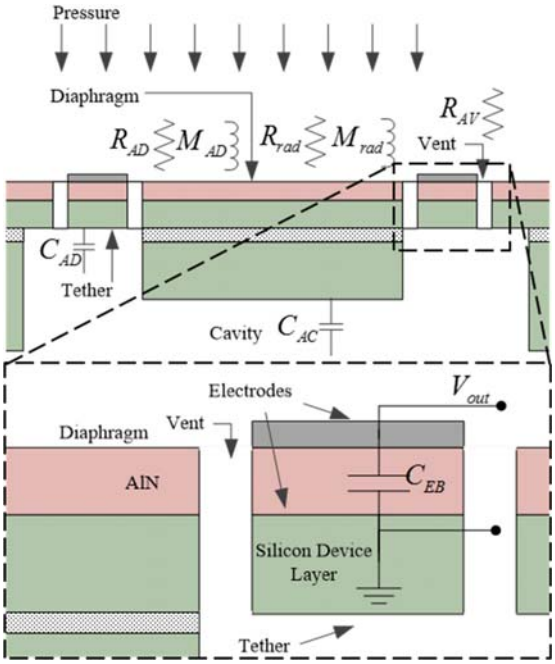

***Figure 5**: Lumped microphone components in the acoustic energy domain (top) and electrical energy domain (bottom*

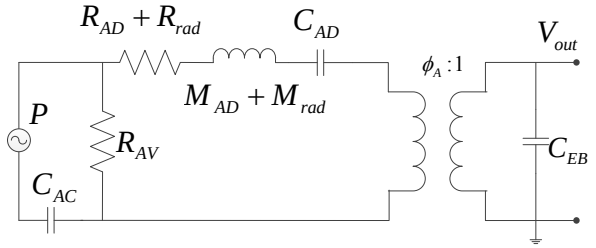

***Figure 6**: Equivalent circuit model of the microphone. Coupling between acoustic and electrical domains is achieved by the transformer.*

where $\forall$ is the volume of the back cavity, ρ_0 is the density of air, and c_0 is the speed of sound in air. The electrical impedance is simply the capacitance created by the AlN dielectric between the top and bottom electrodes (parasitic capacitance neglected), represented by C_{EB}. To couple the acoustic energy domain to the electrical energy domain we use a transformer with the transduction factor $\emptyset_A$.

The resonant frequency of the device is controlled by the diaphragm mass (M_{AD}) and tether compliance (C_{AD}),

$$f_{res} = \frac{1}{2\pi\sqrt{M_{AD}C_{AD}}} \tag{2}$$

The quality factor (Q) of the device (i.e., the sharpness of the resonant peak, defining the gain at the frequency of interest and relative out-of-band rejection) is also dependent on the mass and compliance of the device. Ignoring the vent resistance and back cavity compliance, the quality factor is given as

$$Q \approx \frac{1}{R_{AD}+R_{rad}}\sqrt{\frac{M_{AD}}{C_{AD}}} \tag{3}$$

Combining (2) and (3) shows that reducing the resonant frequency into the operational bandwidth while maintaining a large quality factor can be accomplished by increasing the mass while keeping the tether compliance constant. However, the additional mass causes the device to become more sensitive to undesirable environmental vibrations.

An equivalent circuit model (Figure 6) is generated using the lumped elements shown in Figure 5. This model provides first principle insights into the device operation.

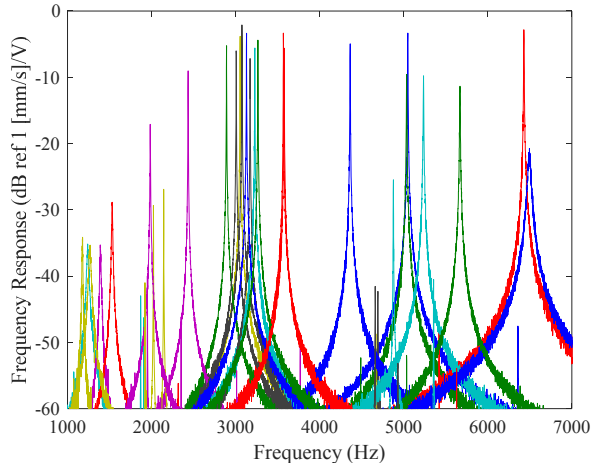

***Figure 7**: Frequency response measurements of a subset of multiple microphone designs in air obtained via a laser vibrometer.*

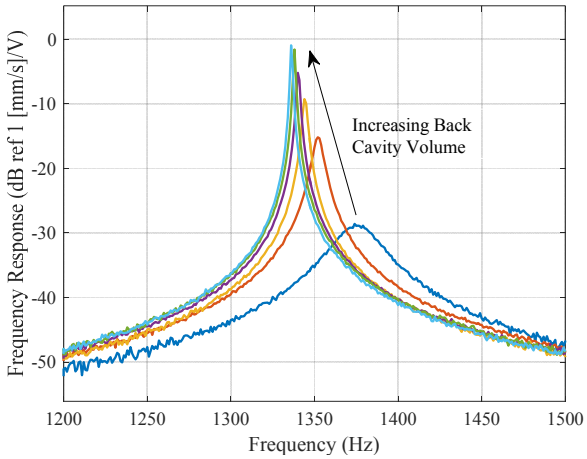

***Figure 8**: Frequency response of a single resonant microphone with increasing back cavity volume measured via laser vibrometer.*

As observed in the equivalent circuit, the vent resistance (R_{AV}) and back cavity compliance (C_{AC}) create a high-pass filter which determines the cut-on frequency of the microphone. This generally defines the lower bound of the operational bandwidth; however, in the present device, back cavity manipulation allows us to lower the cut-on frequency so as not to dampen the device Q. The back cavity effect on resonant microphone performance is investigated in the following characterization section.

CHARACTERIZATION

The microphones are first characterized using a laser vibrometer (LV) which uses optical interferometry to measure the velocity at a user defined location (in this case on the diaphragm). Because piezoelectrics are reciprocal we can apply a voltage between the top and bottom electrodes and measure the diaphragm vibrational response with the LV. The LV system was used to obtain the frequency response of each microphone design over a large range of frequencies. A subset of results is shown in Figure 7. As observed, the sensitivity of the devices tends to increase with increasing frequency for a fixed back cavity volume due to the vent-back cavity high pass filter discussed previously. Microphones were obtained with resonant frequencies ranging from 430 Hz to over 10 kHz with quality factors up to 3000.

The LV system was also used to investigate the effects of the back cavity size on the device performance. The results are shown in Figure 8. As the back cavity volume increases the quality factor also increases while the frequency of the resonant peak decreases. This is due to the coupling of the vent resistance, R_{AV}, with the compliance of the back cavity, C_{AC}, to create a high-pass filter (as discussed previously). The compliance of the back cavity is increased by growing its volume, lowering the cut-on frequency of the high-pass filter. Simultaneously, decreasing the size of the back cavity causes a reduction in stiffness of the diaphragm which tends to reduce the frequency of the resonant peak.

The microphones are packaged using a transimpedance amplifier for signal conditioning. The transimpedance circuit bypasses the parasitic capacitance

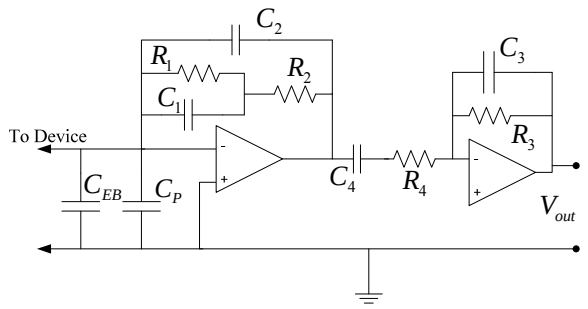

***Figure 9**: Transimpedance amplifier circuit used to bypass the device parasitic capacitance. Transimpedance amplification is removed in all subsequent results.*

formed by the traces and bondpads over the uniformly doped silicon device layer. Future device design iterations will use a patterned implant to reduce parasitic capacitance.

The packaged device is placed in a plane wave tube (PWT) for acoustic testing. At one end of the PWT is a speaker which outputs oscillatory pressure waves which travel as plane waves down the length of the tube. At the other end of the tube the device under test (DUT) and reference microphone are located on a common plane such that both experience a common pressure. The PWT testing setup is shown in Figure 10. The acoustic frequency response of a selected device is shown in Figure 11. The peak response gives an open-circuit (i.e. with the transimpedance amplification removed) sensitivity of 600 mV/Pa. In Figure 11 we also observe a spurious peak approximately 30 dB below the primary peak. This spurious response results from a tilting resonant mode as observed by finite element analysis as shown in Figure 12.

SUMMARY

In this work, resonant MEMS microphones based on piezoelectric AlN were developed to create passive, acoustic filters. The piezoelectric microphones require no power to operate and are intended use in a near-zero power wakeup system combining the device discussed within with low-power CMOS circuitry. Unlike general microphones, these devices were designed to operate around their resonant frequency. Microphones were demonstrated with resonant frequencies ranging from 430 Hz to over 10 kHz while demonstrating quality factors up to 3000. Open-circuit voltages exceeding 600 mV/Pa were obtained. Future work will combine these zero-power

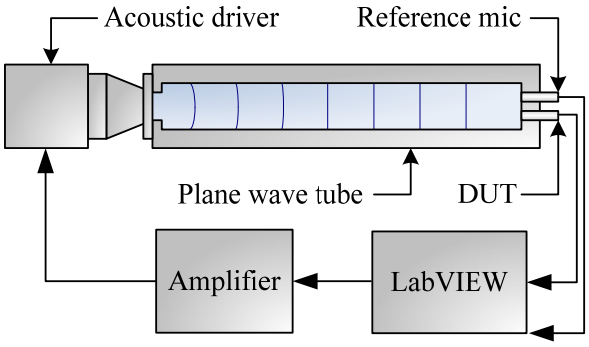

***Figure 10**: Plane wave tube testing setup showing the device under test and reference microphone.*

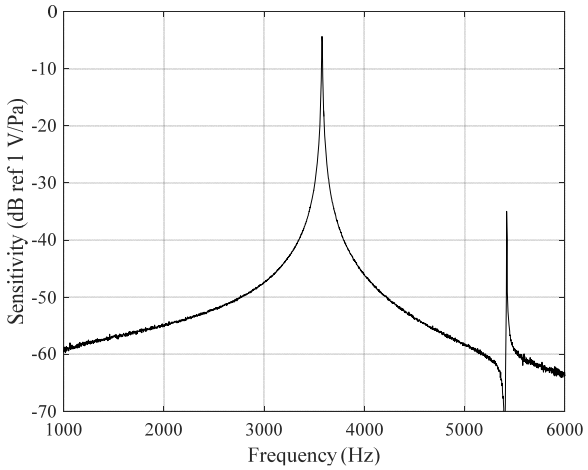

***Figure 11**: Open-circuit sensitivity of a select resonant microphone tested in an acoustic plane wave tube. Peak occurs at 3500 Hz with 600 mV/Pa sensitivity.*

sensors with very-low-power ASIC CMOS chips to create a near-zero power wakeup system.

ACKNOWLEDGEMENTS

This work was supported by the Laboratory Directed Research and Development (LDRD) program at Sandia National Laboratories. Sandia National Laboratories is a multi-program laboratory managed and operated by Sandia Corporation, a wholly owned subsidiary of Lockheed Martin Corporation, for the U.S. Department of Energy's National Nuclear Security Administration under contract DE-AC04-94AL85000. The authors acknowledge fabrication support by the Sandia MESAFab operations team, especially T. Young and S. Summers and test and measurement support by R. McClanahan, J. Stevens, A. Young, and S. Lemon.

REFERENCES

[1] S. Trolier-McKinstry and P. Muralt, "Thin Film Piezoelectrics for MEMS," *Journal of Electroceramics*, vol. 12, no. 1-2, pp. 7-17, 2004.

[2] D. T. Blackstock, *Fundamentals of Physical Acoustics*. New York: Wiley-Interscience Publication, 2000.

CONTACTS

*B. A. Griffin, tel (505) 844-7370: bagriff@sandia.gov

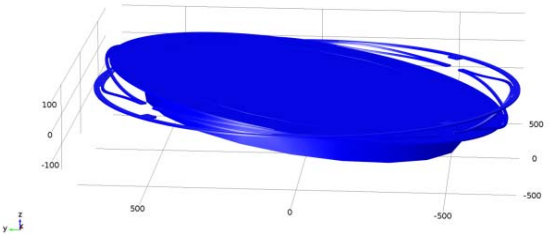

***Figure 12**: Finite element model results showing the secondary tilting mode.*